Journal of Alloys and Compounds 726 (2017) 758–764

Contents lists available at ScienceDirect

Journal of Alloys and Compounds

journal homepage: http://www.elsevier.com/locate/jalcom

On the edge of periodicity: Unconventional magnetism of $Gd_{117}Co_{56.4}Sn_{114.3}$

J. Liu [a, b, 1], Y. Mudryk [a, *], D.H. Ryan [c], V.K. Pecharsky [a, b]

[a] Ames Laboratory, U.S. Department of Energy, Iowa State University, Ames, IA, 50011-3020, USA
[b] Department of Materials Science and Engineering, Iowa State University, Ames, IA, 50011-2300, USA
[c] Physics Department and Center for the Physics of Materials, McGill University, 3600 University Street, Montreal, Quebec, H3A 2T8, Canada

ARTICLE INFO

Article history:
Received 6 June 2017
Received in revised form
1 August 2017
Accepted 2 August 2017
Available online 4 August 2017

Keywords:
Rare earth alloys and compounds
Magnetization
Magnetic frustration
Heat capacity
Mössbauer

ABSTRACT

Magnetization measurements reveal the onset of magnetic ordering at $T_C = 65$ K followed by three additional magnetic anomalies at $T_1 = 47$ K, $T_2 = 28$ K, and $T_3 = 11$ K in $Gd_{117}Co_{56.4}Sn_{114.3}$ – a compound with a giant cubic unit cell that crystallizes in the $Dy_{117}Co_{56}Sn_{112}$ structure type with space group $Fm\bar{3}m$ and lattice parameter $a = 30.186$ Å. The magnetic ordering temperature increases with applied magnetic field; however, the analysis of magnetic data indicates that antiferromagnetic interactions also play a role in the ground state. AC magnetic susceptibility confirms multiple magnetic anomalies and shows minor frequency dependence. The local magnetic ordering below 60 K is supported by the Mössbauer spectroscopy. A single broad anomaly is detected at T_3 in the heat capacity; we suggest that magnetic domains form below this temperature. These data highlight unique features of magnetism in this and, potentially, other rare-earth intermetallics crystallizing with giant unit-cells where the exchange correlation lengths are much shorter when compared to the periodicity of the crystal lattice.

1. Introduction

Much of the excitement in nanoscience is related to the fact that properties of a crystalline material may be vastly different when its linear dimensions (e.g. the size of a particle) are reduced from a few micrometers or greater to a few nanometers. Various magnetic nanomaterials have been successfully created by using either the bottom-up or top-down approaches [1,2]. Common and well-known problems in nanoscience include size uniformity and reproducibility, scale-up of synthesis, and, for non-oxide materials, keeping oxygen away from the particle surfaces, among others. Considering that most useful magnetic nanoparticles (e.g. for exchange spring magnets) must be reduced to a few nanometers in size [3,4], and that typical unit cell dimensions of a magnetic crystal are between 5 and 10 Å, a cube-like nanoparticle with 3 nm sides, will consist of ~30–~200 unit cells. Assuming a defect-free nanoparticle, periodicity is short lived, being broken at the particle boundaries every 3 to 6 unit cells. Now take a crystal that has a unit cell comparable to a 3 nm small particle. What would normally be a collection of a few tens to a few hundreds of identical unit cells now becomes a nearly perfectly ordered assembly of a few thousands of atoms but with periodicity at the length scale of a typical nanoparticle. It is, therefore, reasonable to expect that properties of such a crystal in bulk form would be fundamentally different from the properties of both conventional crystalline materials with “normal” unit cells and nanoparticles.

Research on intermetallic compounds with giant unit cells dates back to 1944 when Perlitz reported an extremely large cubic unit cell for the β phase in the Al-Mg system, which has a lattice parameter of $a = 28.13$ Å [5]. This phase with Mg_2Al_3 composition is also known as one of the so-called Samson phases named after the scientist who first reported its very complex crystal structure in 1965 [6]. A few years earlier Samson determined another crystal structure with a similarly large cubic unit cell ($a = 30.56$ Å) containing in excess of 1000 atoms in a compound with the composition $NdCd_{1.92}$ [7]. More systematic research on such systems started recently [8–13], when both high-resolution x-ray diffraction and transmission electron microscopy instruments became readily available.

Reminiscent of nanocrystals, giant unit cells are constructed from smaller structural blocks or clusters and they may be viewed as cluster-modulated structures [14]. For example, a number of

* Corresponding author.
E-mail address: slavkomk@ameslab.gov (Y. Mudryk).
[1] Current affiliation: Seagate Technology, Bloomington, MN, USA.

http://dx.doi.org/10.1016/j.jallcom.2017.08.009
0925-8388/

related compounds with giant unit cells found in the Al-Cu-Ta system show the so-called super-ordering of fundamental Laves phase-type structural blocks with a common periodicity of ~6.5 Å [13], while the structure of $YbCu_{4.5}$ consists of $AuBe_5$-type blocks (a ~7 Å) [8]. Very subtle changes in chemistry (a few at. %) may drastically change the size of the unit cell, as was observed in the Al-Cu-Ta, Yb-Cu, and Dy-Cu systems [9,11,13]. Structurally distorted regions occur in many compounds with giant unit cells where highly symmetrical atomic environment coexists with distorted polyhedra and partially occupied atomic sites [6–8,13].

In the ternary intermetallic R-T-X systems (R = rare earth, T = transition metal, X = p-element) an extended family of nearly isostructural compounds, all adopting giant cubic unit cells with a on the order of 30 Å, shows highly complex crystal structures and physical behavior. The first compound reported to crystallize with the giant unit cell is $Tb_{117}Fe_{52}Ge_{112}$ [15]. Since then, a series of compounds with the $Tb_{117}Fe_{52}Ge_{112}$ − type structure has been prepared and characterized with X = Ge: $R_{117}Fe_{52}Ge_{112}$ (R = Y, Pr, Sm, Gd-Tm and Lu), $R_{117}Cr_{52}Ge_{112}$ (R= Nd and Sm) and $R_{117}Co_{52}Ge_{112}$ (R= Pr and Sm) [16–19]. Similar compounds were found with X = Sn, and a closely related crystal structure, where one additional site is fully or partially occupied by the Co atoms, was first reported for $Dy_{117}Co_{57}Sn_{112}$ [20]. Recently, $R_{117}Co_{54+x}Sn_{112\pm y}$ compounds were reported for R = Y, La − Lu, except Pm, Eu and Yb [21–25]. The Co/Sn ratio varies slightly depending on the size of the R component [24]. Different degrees of crystallographic disorder have been reported for most $R_{117}Co_{54+x}Sn_{112\pm y}$ compounds [22,24,25]. Single crystals of $R_{117}Ni_{54-y}Sn_{112-z}$ compounds with R = Gd, Tb, Dy obtained by flux growth method showed much disorder as well [26].

The physical properties of these compounds are not well understood, but several recent studies report basic magnetic and transport properties mainly for $R_{117}Co_{54+x}Sn_{112\pm y}$ alloys [22–27], but also for $Tb_{117}Fe_{52}Ge_{113.8(1)}$ [28], and $R_{117}Ni_{54-y}Sn_{112-z}$ [26]. The presence of chemical and structural disorder and the fact that these systems are on the edge of breaking translational symmetry leads to predominantly glassy behavior. For example, cluster spin glass ground states have been observed in $Pr_{117}Co_{54.5}Sn_{115.2}$ [27] and $Tb_{117}Fe_{52}Ge_{113.8}$ [28], and an exceptionally low lattice thermal conductivity was reported for a single crystal of $Gd_{117}Co_{56}Sn_{112}$ [23].

The magnetic and transport properties of $Gd_{117}Co_{56}Sn_{112}$ were measured using a flux-grown single crystal [23] but it was found that properties of bulk polycrystalline samples of $Gd_{117}Co_{56.4}Sn_{114.3}$ are somewhat different from those of the single crystal [24]. For example, the bulk material exhibits several magnetic anomalies in a 1 kOe applied magnetic field, which were not observed in the single crystal [23]. In addition, $Gd_{117}Co_{56.4}Sn_{114.3}$ polycrystalline samples show a clear anomaly in the temperature dependence of electrical resistivity around 70 K [24]. A similar anomaly was observed in a single crystal but at a much lower temperature (near 10 K) [23]. The differences between the physical behavior of single- and polycrystalline samples was suggested to originate from structural and/or compositional imperfections that are inherently present in such complex systems [24].

In this work we report the study of $Gd_{117}Co_{56.4}Sn_{114.3}$ using detailed dc and ac magnetization measurements, heat capacity measurements, and Mössbauer effect, all of which have revealed unexpected physics that may be linked to competition between long-range and short-range magnetic interactions in $Gd_{117}Co_{56.4}Sn_{114.3}$.

2. Experimental methods

The sample of $Gd_{117}Co_{56.4}Sn_{114.3}$ used in this study was prepared by arc melting and annealing in a helium-filled quartz ampoule at 1050 °C for 15 days. The results presented here were obtained on the same sample that was used in Ref. [24] where the details of x-ray diffraction study and crystal structure can be found (also see Table 1). A second sample of the same composition was synthesized to validate the observed experimental results confirming they are reproducible.

Magnetic measurements were performed using a superconducting quantum interference device (SQUID) magnetometer (MPMS XL, Quantum Design, USA). The dc magnetization was measured in the temperature range of 2–300 K and a magnetic field range of 0–70 kOe in zero-field-cooled (ZFC) warming regime followed by the field-cooling (FC) measurements. The AC magnetic susceptibility was measured in an AC field of 5 Oe at frequencies varying from 1 to 1000 Hz in the temperature range of 2–150 K in zero dc applied field first, then with a constant frequency 1 Hz in different dc bias magnetic fields between 0 and 10 kOe. Heat capacity was measured on a zero field cooled sample upon heating using Physical Property Measurement System (PPMS) in zero and 10 kOe magnetic fields in the temperature range between 2 and 80 K.

The 50 mCi ^{155}Gd source and sample were mounted vertically in a helium flow cryostat and the Mössbauer drive was operated in sinusoidal mode. The 86.55 keV Mössbauer γ-photons were isolated from the various x-rays emitted by the source with a high-purity Ge detector. The system was calibrated using a laser interferometer with velocities cross-checked against both ^{57}CoRh/α-Fe at room temperature and $^{155}SmPd_3/GdFe_2$ at 5 K. The ^{155} Gd Mössbauer spectra were fitted using a non-linear least-squares minimization routine with line positions and intensities derived from an exact solution to the full Hamiltonian [29].

3. Results and discussion

3.1. Magnetic susceptibility

The magnetization of $Gd_{117}Co_{56.4}Sn_{114.3}$ measured in ZFC and FC regimes at 100 Oe is shown in Fig. 1. A sharp increase of magnetization at 65 K (T_C) marks the transition from the paramagnetic (PM) to the magnetically ordered state. A broad peak at $T_1 = 47$ K followed by the steep decrease in magnetization indicates the prevalence of antiferromagnetic interactions in the low-temperature state of $Gd_{117}Co_{56.4}Sn_{114.3}$. Two additional anomalies: a change of slope at $T_2 = 28$ K, (better seen as a peak in the dM/dT plot shown in the inset of Fig. 1), and a minor peak at $T_3 = 11$ K are also observed in both ZFC and FC plots. Usually such anomalies are associated with spin reorientation. As discussed in Ref. [24], the multiple magnetic structures are expected in $Gd_{117}Co_{56.4}Sn_{114.3}$ considering its complex crystal structure where eight crystallographically non-equivalent atomic sites are occupied by the Gd atoms. At the same time, the changes in magnetization may be related to the

Table 1
Physical parameters of the $Gd_{117}Co_{56.4}Sn_{114.3}$ compound.

Parameter	Value	Reference
Lattice parameter, a	30.186(4) Å	[24]
	30.159(3) Å	[23]
Magnetic ordering temperature, T_C	65 K	This study
T_1	47 K	This study
T_2	28 K	This study
T_3	11 K	This study
Effective magnetic moment, p_{eff}	7.1 μ_B/Gd	[24]
	7.1 μ_B/Gd	This study
Weiss temperature, θ_p	87 K	[24]
	89 K	This study

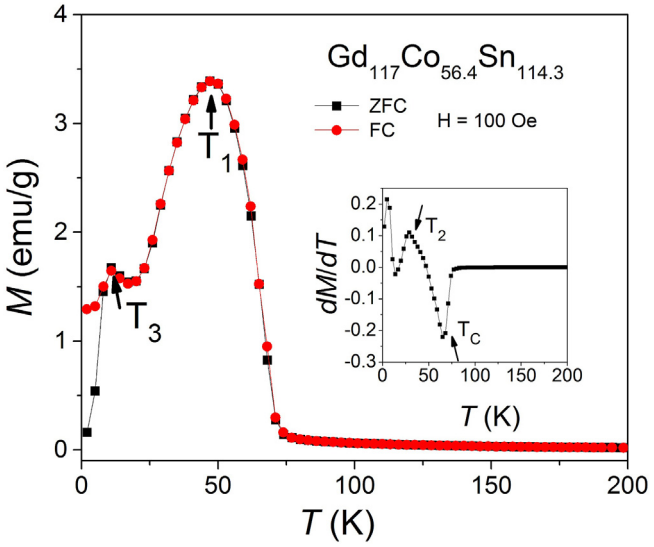

Fig. 1. Magnetization of $Gd_{117}Co_{56.4}Sn_{114.3}$ measured as a function of temperature in 100 Oe magnetic field under ZFC and FC conditions. The inset is the first derivative of magnetization with respect to the temperature.

cluster structure of the compound. Because the nearest neighbor environment of the clusters is different, the temperature variation of magnetic interactions within a cluster as well as the interactions between the clusters can lead to the unusual thermomagnetic behavior observed in Fig. 1. Thermomagnetic irreversibility in the ZFC warming – FC cooling magnetization data is evident below T_3, and it can be either caused by the domain wall pinning effect (long-range order scenario) or by strong magnetic frustration (glassy behavior). Since irreversibility occurs only at low temperatures, well below the magnetic ordering transition at T_C, the former scenario is more plausible. On the other hand, magnetic frustration is to be expected in this system considering the spin-glass behavior of the $Pr_{117}Co_{54.5}Sn_{115.2}$ [27].

Fig. 2a shows the ZFC and FC M(T) data of $Gd_{117}Co_{56.4}Sn_{114.3}$ measured in magnetic fields of 5, 10, and 30 kOe. The Curie-Weiss fit of the 5 kOe data measured after zero field cooling (Fig. 2b) leads to the effective magnetic moment of 7.1 μ_B/Gd atom and Weiss temperature of 89 K, both of which are practically identical to those reported in Ref. [24]. When the applied magnetic field increases, the anomaly at T_3 practically disappears, and the other magnetic anomalies become broader compared to low magnetic field measurements (especially the one at T_C) and shift to higher temperature. At 30 kOe, the peak at T_1 is fully suppressed and M(T) only exhibits a minor change of slope at ~ 60 K. Magnetic ordering temperature (T_C, defined as the minimum of dM/dT) is remarkably sensitive to the applied magnetic field, rising from ~65 K for $H = 100$ Oe to ~100 K for $H = 30$ kOe. Fewer anomalies are seen in the M(T) behavior as the magnetic field increases suggesting that higher fields make the magnetic interactions more uniform. While alignment of magnetic moments along the magnetic field vector could be another possible explanation for the disappearance of minor magnetic transitions, the M(H) measurements below show that this is not the case here.

Fig. 3 shows magnetization isotherms measured at selected temperatures from 0 to 70 kOe. At 2 K, the magnetization changes nonlinearly with magnetic field but shows no sign of saturation. No hysteresis is observed during increasing and decreasing cycles of the magnetic field. At 50 and 55 K, a weak initial increase in

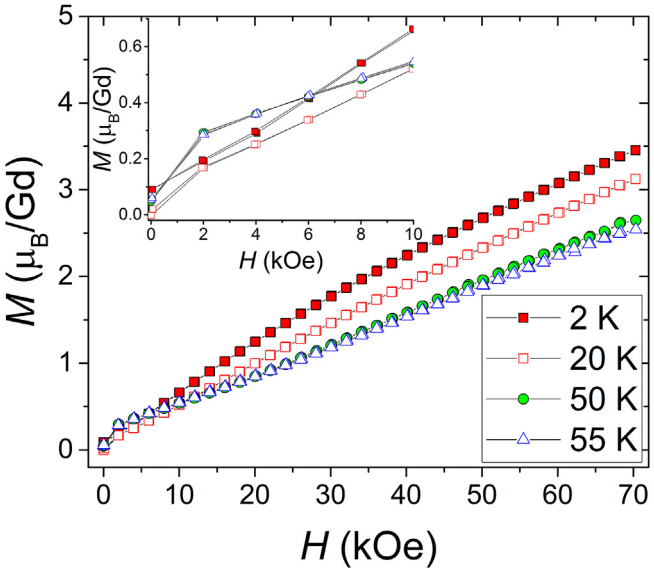

Fig. 3. Isothermal magnetization of $Gd_{117}Co_{56.4}Sn_{114.3}$ measured at 2, 20, 50, and 55 K. The inset magnifies a low-field region between 0 and 10 kOe.

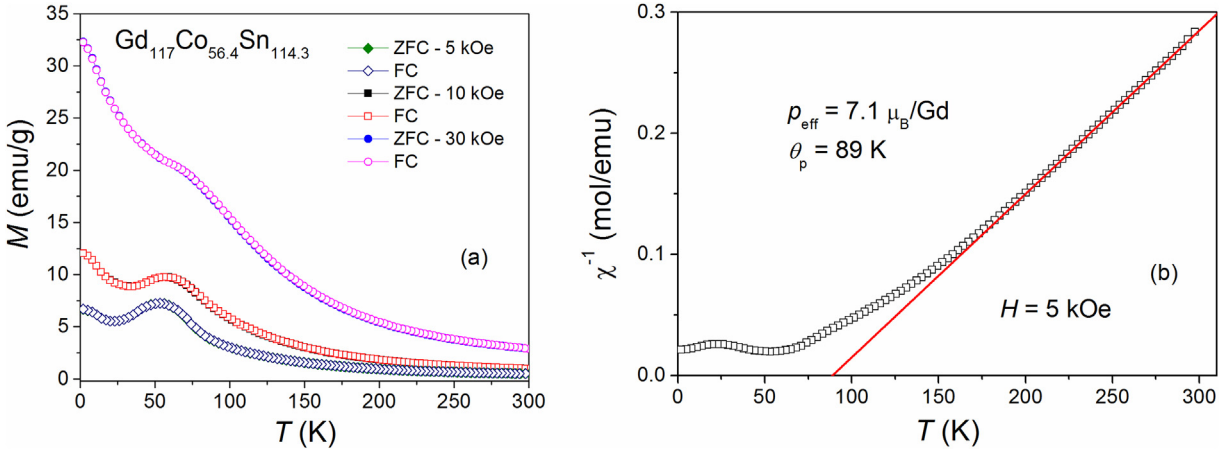

Fig. 2. (a) Temperature dependence of $Gd_{117}Co_{56.4}Sn_{114.3}$ magnetization measured in 5, 10, and 30 kOe magnetic field under ZFC and FC conditions. Note that the ZFC data (filled symbols) completely overlap with the FC data (open symbols) indicating no hysteresis. (b) The inverse magnetic susceptibility (H/M) of $Gd_{117}Co_{56.4}Sn_{114.3}$ measured in a 5 kOe magnetic field after zero field cooling and the Curie-Weiss fit of the data above 200 K.

magnetization is observed for the fields less than 2 kOe, revealing the occurrence of spontaneous magnetization due to the formation of ferromagnetic clusters, consistent with the M(T) data. Overall, the M(H) behavior indicates a dominance of antiferromagnetic interactions with the minor ferromagnetic component.

Fig. 4 shows the temperature dependence of the real χ' and imaginary χ'' parts of the AC susceptibility of $Gd_{117}Co_{56.4}Sn_{114.3}$ sample measured as a function of temperature at frequencies ranging from 1 to 1000 Hz using the AC driving field of 5 Oe. The real part of the susceptibility shows a fast increase starting from ~70 K (i.e. just above T_C), which is typical for the transition from the paramagnetic to the long-range ordered state, and a rounded maximum at ~47 K (T_1), which agrees well with the dc $M(T)$ data. Two other anomalies, a slope change at ~28 K (T_2) and a sharp step at 8 K (near T_3) are observed. Weak frequency dependence occurs from 28 to 8 K but is absent below 8 K, which means that the magnetic irreversibility observed in M(T) data (Fig. 1) below T_3 is caused by coercivity, not magnetic frustration, supporting the hypothesis of magnetic domain formation. In the imaginary part, a sharp step is observed at the Curie temperature. However, this step nearly disappears when the frequency reaches 1000 Hz. The peak observed at 50 K in χ' corresponds to the quick rise of χ'' at this temperature. There is also a peak in χ'' and a change of slope in χ' at 28 K. In addition, χ''(T) shows a small rounded peak at ~14 K followed by a sharp drop. Weak frequency dependence is observed in χ''(T) data between 14 and 28 K.

Fig. 5 shows $\chi'(T)$ and $\chi''(T)$ data of $Gd_{117}Co_{56.4}Sn_{114.3}$ measured in the dc bias magnetic fields of 0, 100, 200, 500, 1000, and 10,000 Oe. Increasing the bias dc magnetic field from 100 to 500 Oe suppresses both the χ' and χ''. The $\chi'(T)$ data show that the 100 Oe external bias dc magnetic field has no significant influence on T_C and T_1 transitions while the anomaly at 8 K develops into a sharp peak. However, the χ''(T) data measured at $H = 100$ Oe only shows peaks at 12 and 36 K, respectively. At $H = 200$ Oe, the T_1 peak shifts remarkably to 40 K and at $H = 500$ Oe, the anomaly at T_1 is not observed, and only the peak at T_C is preserved. At $H = 1$ kOe and above, both χ'(T) and χ''(T) become low even though the magnetization (from M(H)) is not saturating. However, it is expected that the magnetic domains do not respond to the low H_{ac} value (5 Oe) when the dc bias field is $\geq$ 1 kOe.

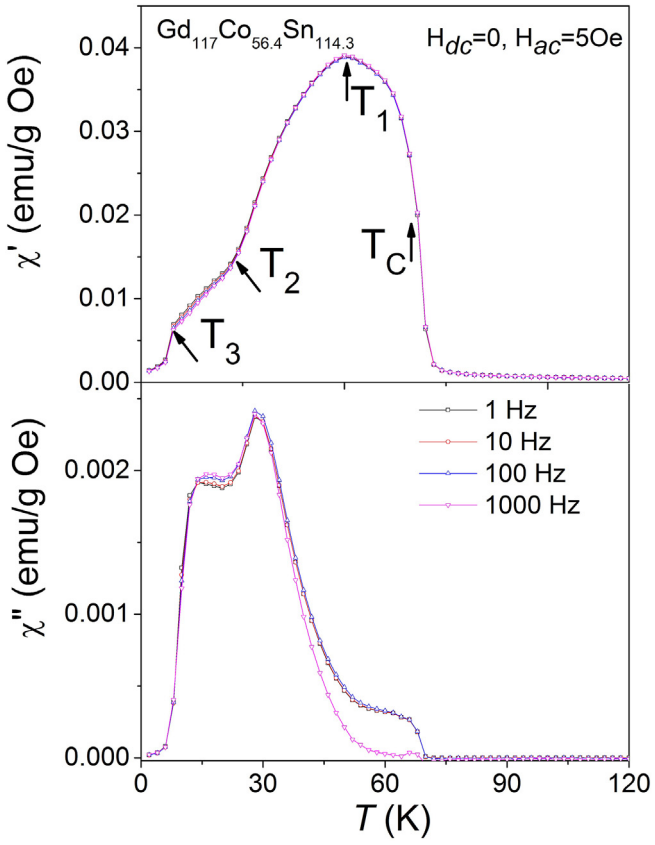

Fig. 4. Temperature dependence of the real (χ') and imaginary (χ'') components of the ac susceptibility between 2 and 120 K at frequencies varying from 1 to 1000 Hz.

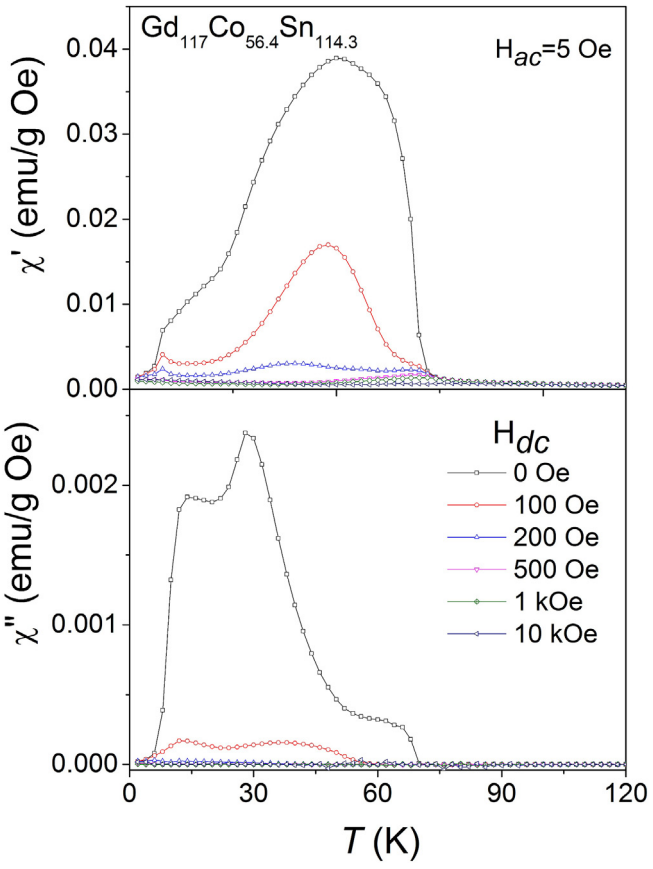

Fig. 5. Temperature dependence of the real (χ') and imaginary (χ'') components of the ac susceptibility between 2 and 120 K recorded with different H_{dc}.

It is somewhat surprising that the ac magnetic susceptibility of $Gd_{117}Co_{56.4}Sn_{114.3}$ shows only weak frequency dependence, when much stronger frequency dependence related to cluster spin glass behavior is observed in the isostructural compound $Pr_{117}Co_{54.5}Sn_{115.2}$ [27] as well as in the structurally similar $Tb_{117}Fe_{52}Ge_{113.8}$ [28]. It is known that structural disorder is present in all of these compounds. Random occupation of Co and Sn in some of the atomic sites [24] affects nearest neighbor environment and frustrates the indirect exchange interaction of R atoms mediated by conduction electrons. These two features, crystallographic disorder and magnetic frustration, are the two key ingredients for the formation of a spin glass state. However, in $Gd_{117}Co_{56.4}Sn_{114.3}$ the spin glass state is not observed as follows from the nearly frequency independent AC magnetic susceptibility. Conversely, magnetic measurements indicate the possibility of ferromagnetic long range magnetic ordering supported by the clearly positive Weiss constant, $\theta_p = 89$ K (Fig. 2b and Table 1). The difference between Gd and Pr compounds may originate from the fact that the average interatomic distances are shorter in $Gd_{117}Co_{56.4}Sn_{114.3}$

(a = 30.186 Å, see Table 1) compared to $Pr_{117}Co_{54.5}Sn_{115.2}$ (a = 30.8295 Å [27]). Further, in R_2TX_3 compounds (R = U or rare earth element, T = transition metal, X = Si, In and Ge) with AlB_2- or $CaIn_2$-type crystal structure, long range ordering, spin glass, or coexistence of both long range and spin glass states are known to occur depending on the strength of the magnetic exchange interaction as R, T, or X vary [30]. One can expect similar variation to occur in $R_{117}Co_{54+x}Sn_{112\pm y}$ compounds.

3.2. Heat capacity

The heat capacity of $Gd_{117}Co_{56.4}Sn_{114.3}$ was measured in zero and 10 kOe magnetic fields and the results are shown in Fig. 6. Except for a broad anomaly at ~10 K, there are no obvious signatures of phase transformations in the heat capacity plot despite the fact that the multiple anomalies were observed in the M(T) data. Usually, the absence of heat-capacity anomaly at the magnetic phase transition indicates the absence of the conventional long-range magnetic ordering and the formation of a spin glass or a frozen state [31–33]. However, in $Gd_{117}Co_{56.4}Sn_{114.3}$ the frequency dependence is minor and mostly observed in χ''(T) (Fig. 4). Further, the electrical resistivity shows a clear anomaly in $Gd_{117}Co_{56.4}Sn_{114.3}$ compound around T_C [24], also shown as inset in Fig. 6. The lack of distinct heat-capacity anomalies indicates that the entropy changes associated with the changes in the spin structure of $Gd_{117}Co_{56.4}Sn_{114.3}$ are negligible compared to the phonon contribution to the heat capacity. Additionally, it appears that the magnetic entropy is spread over an unusually broad range of temperatures. This is partially supported by the fact that the applied magnetic field affects the heat-capacity in the very broad temperature range starting above ~30 K, indicating a major contribution from magnetic entropy below, at, and above T_C. According to the inverse magnetic susceptibility plot (H/M *vs. T*, Fig. 2b, see also Ref. [24]) the deviation from the linear Curie-Weiss behavior begins around 150 K, where the *conventional* short-range clustering likely begins.

However, the discrepancy between electrical transport and heat capacity data is not easy to explain. One may assume that the magnetic ordering of $Gd_{117}Co_{56.4}Sn_{114.3}$ *begins* at T_C with a local ordering of one or more clusters, sufficient to modify electrical resistivity behavior, and *ends* either at T_2 ~28 K or T_3 ~11 K – it appears that magnetic domains exist below T_3. This would be quite an unusual behavior for a normal intermetallic compound, however, in the system where the lattice parameter (a measure of crystallographic periodicity) by far exceeds the range of the RKKY exchange correlations that govern the magnetism of rare-earth compounds one may expect that the true long-range magnetic order is not established across the whole unit-cell at once. Traditionally such phenomenon would be described as a short-range order effect (e.g. a spin glass or a cluster spin glass), but more likely than not the size of the magnetically ordered clusters is so large that their ordering exhibits at least some characteristics of conventional long-range order.

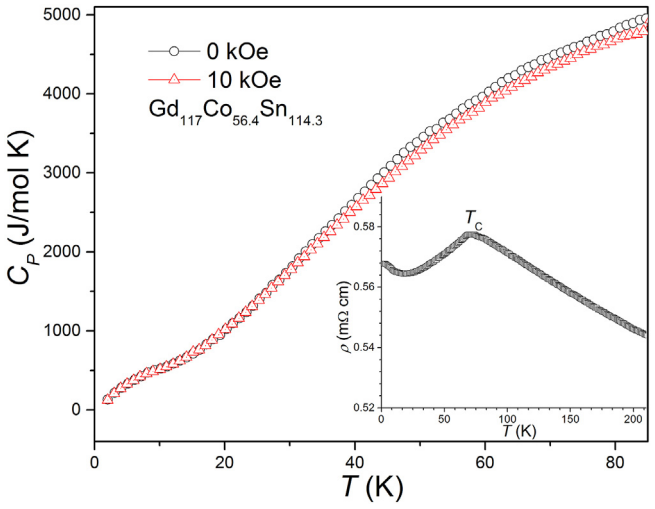

Fig. 6. Temperature dependence of heat capacity of $Gd_{117}Co_{56.4}Sn_{114.3}$ under zero and 10 kOe magnetic field. Temperature dependence of electrical resistivity (from Ref. [24]) is shown in the inset for comparison.

3.3. Mössbauer effect

In order to further probe the magnetic ordering in $Gd_{117}Co_{56.4}Sn_{114.3}$, ^{155} Gd Mössbauer spectra were recorded between 5 K and 60 K (the upper limit being set by the rapid reduction in the recoil-free fraction at high temperatures). The spectra shown in Fig. 7 exhibit few resolved features as a result of the severe line overlap that results from the many crystallographically distinct gadolinium sites in the large unit cell. However some conclusions

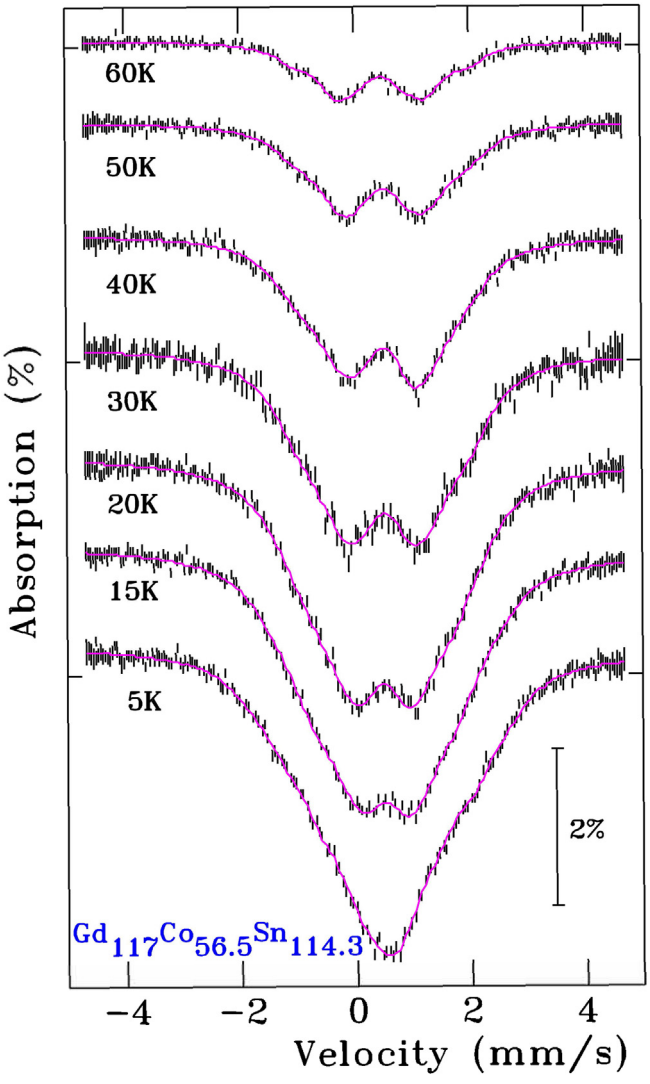

Fig. 7. ^{155}Gd Mössbauer spectra for $Gd_{117}Co_{56.4}Sn_{114.3}$ measured between 5 and 60 K. The solid lines are fits described in the text.

can be drawn from a visual inspection: at 60 K the form of the spectrum suggests that the gadolinium is paramagnetic, while the broadening that occurs on cooling clearly indicates the development of magnetic order.

Given the severe line overlap and multiple gadolinium sites, a free fit was not likely to be stable, so we sought simplifying constraints. Assuming that the 60 K pattern was indeed paramagnetic we identified the minimum number of doublets that would fit the observed spectral shape. The strongest doublet is clear, and there are visible shoulders due to a second doublet with a larger splitting. A third, weaker doublet was found to be necessary to account for a mis-fit in the center of the pattern. This final fit gave a χ^2 of 0.98 and a linewidth of 0.36(2) mm/s (FWHM) typical of ^{155} Gd Mössbauer spectra. The three components had quadrupole splittings (eQV_{zz}) and areas of: 1.79(14) mm/s (32(5)%), 3.38(12) mm/s (47(4)%) and 6.30(13) mm/s (21(2)%). These were rounded to 3:5:2 and used as constraints on eQV_{zz} and area for the fits to the lower temperature spectra.

The results of fitting this constrained three-site model are shown as the solid lines in Fig. 7, and the fitted hyperfine fields for the three components are shown as a function of temperature in Fig. 8. Even with the area and quadrupole constraints, it is apparent that the scatter remains significant, and it is unlikely the fits are unique, however the trends are still clear. The average hyperfine field ($<B_{hf}>$, shown as an inset to Fig. 8) shows evidence for two magnetic transitions: The appearance of a hyperfine field on cooling through 60 K, and a break in $<B_{hf}>$ vs. (T) near 20 K. The former corresponds to T_C, while the latter to T_2. While the assignment of the 60 K event to the onset of order is quite robust, the severe line overlap and the limited basis for the constrained fits make it difficult to establish the nature of the 20 K event. The change in spectral shape is suggestive of a reduction in the projection of B_{hf} onto the principal axis of the electric field gradient, which would imply a spin reorientation occurs on cooling through 20 K, but this assignment remains speculative without independent confirmation.

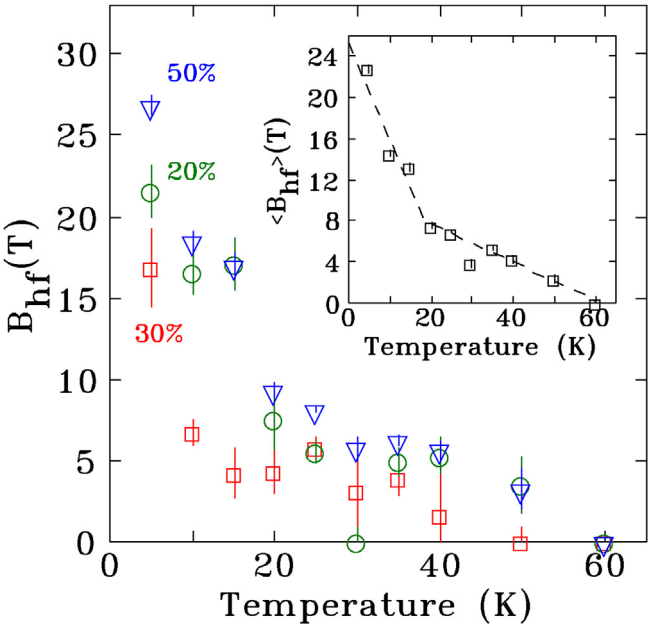

Fig. 8. Temperature dependence of the hyperfine field at the three sites fitted to the spectra shown in Fig. 7. The area ratios were constrained to 50% (blue triangles), 30% (red squares), and 20% (green circles) based on the 60 K spectrum. The inset shows the average hyperfine field with a dashed guide to the eye showing the break at ~20 K. (For interpretation of the references to colour in this figure legend, the reader is referred to the web version of this article.)

4. Conclusions

The physical behavior of $Gd_{117}Co_{56.4}Sn_{114.3}$ compound is difficult to describe in terms of conventional magnetic ordering due to the fact that short-range order, minor magnetic frustration, and magnetic domains are all present at low temperatures.

Four consecutive magnetic anomalies at $T_C = 65$ K, $T_1 = 47$ K, $T_2 = 28$ K, and $T_3 = 11$ K have been observed in $Gd_{117}Co_{56.4}Sn_{114.3}$ by both dc and ac magnetization measurements. Mössbauer effect study shows that magnetic ordering in $Gd_{117}Co_{56.4}Sn_{114.3}$ sets in around 60 K and another phase transition occurs at 20 K. The ordering temperature, T_C, quickly increases with increasing magnetic field. The temperature of magnetic anomalies is frequency independent according to ac susceptibility, ruling out the possibility of spin glass state; however, a minor frequency dependence of $\chi''(T)$ data suggests some magnetic frustration. The absence of anomalies associated with the multiple phase transitions in the heat capacity data indicates that the entropy change due to the magnetic transition is either negligible or spread out over a large temperature range. At the same time it appears that long range ferromagnetic order (magnetic domains) sets in below T_3 coinciding with the approximate temperature of the broad heat capacity anomaly and near the second transition observed in Mössbauer data.

Acknowledgments

This work was supported by the U.S. Department of Energy (DOE), Office of Science, Basic Energy Sciences, Materials Science and Engineering Division. The research was performed at the Ames Laboratory, which is operated for the U.S. DOE by Iowa State University under contract No. DE-AC02-07CH11358. Financial support for the Mössbauer study was provided by the Natural Sciences and Engineering Research Council of Canada, and the Fonds Québécois de la Recherche sur la Nature et les Technologies. We gratefully acknowledge Raghu Rao and Robert Speranzini for the activation of the ^{155}Gd Mössbauer source in the National Research Universal (NRU) research reactor and Rasa Rejali for the assistance with the collection of the Mössbauer data.

References

[1] X.M. Lin, A.C.S. Samia, Synthesis, assembly and physical properties of magnetic nanoparticles, J. Magn. Magn. Mater. 305 (2006) 100–109.
[2] S. Bedanta, A. Barman, W. Kleemann, O. Petracic, T. Seki, Magnetic nanoparticles: a subject for both fundamental research and applications, J. Nanomater. (2013) 952540.
[3] S. Bader, Colloquium: opportunities in nanomagnetism, Rev. Mod. Phys. 78 (2006) 1–15.
[4] R. Skomski, Nanomagnetics, J. Phys. Condens. Matter 15 (2003) R841–R896.
[5] H. Perlitz, Crystal structure of β-Aluminium-Magnesium alloy, Nature 154 (1944) 606.
[6] S. Samson, The crystal structure of the Phase β–Mg_2Al_3, Acta Cryst. 19 (1965) 401–413.
[7] S. Samson, Crystal structure of $NaCd_2$, Nature 195 (1962) 259–262.
[8] R. Černý, M. François, K. Yvon, D. Jaccard, E. Walker, V. Petříček, I. Cisařová, H.-U. Nissen, R. Wessicken, A single-crystal x-ray and HRTEM study of the heavy-fermion compound $YbCu_{4.5}$, J. Phys. Condens. Mater. 8 (1996) 4485–4493.
[9] R. Černý, L. Guénée, R. Wessicken, A single-crystal x-ray and HRTEM study of new series of compounds $DyCu_x$ ($x = 4.5$, 4 and 3.5), J. Solid State Chem. 174 (2003) 125–131.
[10] M. Feuerbacher, et al., The Samson phase β-Mg_2Al_3, revisited, Z. Krist. 222 (2007) 259–288.
[11] S. Gottlieb-Schönmeyer, S. Brühne, F. Ritter, W. Assmus, S. Balanetskyy, M. Feuerbacher, T. Weber, W. Steurer, Crystal growth of copper-rich ytterbium compounds: the predicted giant unit cells structures $YbCu_{4.4}$ and $YbCu_{4.25}$, Intermetallics 17 (2010) 6–10.
[12] J. Dolinšek, M. Wencka, M. Jagodič, Z. Jagličić, S. Gottlieb-Schönmeyer, F. Ritter, W. Assmuss, Slow-charge-carrier electronic transport in the heavy-

fermion $YbCu_{4.25}$ complex intermetallic, Solid State Comm. 150 (2010) 1629–1632.
[13] T. Weber, J. Dshemuchadse, M. Kobas, M. Conrad, B. Harbrecht, W. Steurer, Large, larger, largest – a family of cluster-based tantalum copper aluminides with giant unit cells. I. Structure solution and refinement, Acta Cryst. B65 (2009) 308–317.
[14] J. Dshemuchadse, D.Y. Jung, W. Steurer, Structural building principles of complex face-centered cubic intermetallics, Acta Cryst. B67 (2011) 269–292.
[15] V.K. Pecharskii, O.I. Bodak, V.K. Bel'skii, P.K. Starodub, I.R. Mokra, E.I. Gladyshevskii, Crystal structure of $Tb_{117}Fe_{52}Ge_{112}$, Kristallografiya 32 (1987) 334–338 (in Russian).
[16] O.Y. Mruz, Dissertation of Candidate of Chemical Science, L'viv State University, Ukraine, 1988 (in Russian).
[17] A.V. Morozkin, Y.D. Seropegin, V.K. Portnoy, I.A. Sviridov, A.V. Leonov, New ternary compounds $R_{117}Fe_{52}Ge_{112}$ (R = Gd, Dy, Ho, Er, Tm) and $Sm_{117}Cr_{52}Ge_{112}$ of the $Tb_{117}Fe_{52}Ge_{112}$-type structure, Mater. Res. Bull. 33 (1998) 903–908.
[18] P.S. Salamakha, Crystal structures and crystal chemistry of ternary rare-earth germanides, in: K.A. Gschneidner Jr., L. Eyring (Eds.), Handbook on the Physics and Chemistry of Rare Earths, vol. 27, Elsevier, Amsterdam, 1999, pp. 225–338. Chap.174.
[19] J. Liu, V. Smetana, K.A. Gschneidner Jr., G.J. Miller, V.K. Pecharsky, J. Appl. Phys. 113 (2013), 17E120(3pp).
[20] P. Salamakha, O. Sologub, G. Bocelli, S. Otani, T. Takabatake, $Dy_{117}Co_{57}Sn_{112}$, a new type of ternary intermetallic stannides with a giant unit cell, J. Alloys Compd. 314 (2001) 177–180.
[21] W. He, J. Zhang, J. Yan, Y. Fu, L. Zeng, Crystal structure and magnetic properties of the new ternary compound $Pr_{117}Co_{57}Sn_{112}$, J. Alloys Compd. 491 (2010) 49–52.
[22] K. Kovnir, M. Shatruk, Magnetism in giant unit cells – crystal structure and magnetic properties of $R_{117}Co_{52+\delta}Sn_{112+\gamma}$ (R = Sm, Tb, Dy), Eur. J. Inorg. Chem. 2011 (2011) 3955–3962.
[23] D.C. Schmitt, N. Haldolaarachchige, Y. Xiong, D.P. Young, R. Jin, J.Y. Chan, Probing the lower limit of lattice thermal conductivity in an ordered extended solid: $Gd_{117}Co_{56}Sn_{112}$, a Phonon Glass-Electron Crystal System, J. Am. Chem. Soc. 134 (2012) 5965–5973.
[24] Y. Mudryk, P. Manfrinetti, V. Smetana, J. Liu, M.L. Fornasini, A. Provino, V.K. Pecharsky, G.J. Miller, K.A. Gschneidner Jr., Structural disorder and magnetism in rare-earth (R) $R_{117}Co_{54+x}Sn_{112\pm y}$, J. Alloys Compd. 557 (2013) 252–260.
[25] P. Chai, M. Abramchuk, M. Shatruck, Synthesis, crystal structure, and magnetic properties of giant unit cell intermetallics $R_{117}Co_{52+\delta}Sn_{112+\gamma}$ (R = Y, La, Pr, Nd, Ho), Crystals 6 (2016), 165(13pp).
[26] L.E. Reyes, R.N. McDougald Jr., G.T. McCandless, M. Khan, D.P. Young, J.Y. Chan, Eutectoid flux growth and physical properties of single crystal $Ln_{117}Ni_{54-y}Sn_{112-z}$ (Ln = Gd-Dy), Cryst. Growth Des. 15 (2015) 295–304.
[27] J. Liu, Y. Mudryk, J.D. Zou, V.K. Pecharsky, K.A. Gschneidner Jr., Antiferromagnetic cluster spin-glass behavior in $Pr_{117}Co_{54.5}Sn_{115.2}$ – a compound with a giant unit cell, J. Alloys Compd. 600 (2014) 101–106.
[28] J. Liu, W. Xie, K.A. Gschneidner Jr., M.G.J. Miller, V.K. Pecharsky, Spin-glass behavior in a giant unit cell compound $Tb_{117}Fe_{52}Ge_{113.8(1)}$, J. Phys. Condens. Matter. 26 (2014), 416003(6pp).
[29] C.J. Voyer, D.H. Ryan, Hyperfine Interact. 170 (2006) 91–104.
[30] D.X. Li, S. Nimori, Y. Shiokawa, Y. Haga, E. Yamamoto, Y. Onuki, Magnetic, transport, and thermal properties of ternary intermetallic compound Nd_2PtSi_3, Solid State Commun. 120 (2001) 227–232.
[31] J.A. Mydosh, Disordered magnetism and spin glasses, J. Magn. Magn. Mater. 157/158 (1996) 606–610.
[32] H. Tang, V.K. Pecharsky, K.A. Gschneidner Jr., A.O. Pecharsky, Interplay between reversible and irreversible magnetic phase transitions in polycrystalline Gd_5Ge_4, Phys. Rev. B 69 (2004), 064410(9pp).
[33] J. Liu, D. Paudyal, Y. Mudryk, J.D. Zou, K.A. Gschneidner Jr., V.K. Pecharsky, Unusual magnetic and structural transformations of $DyFe_4Ge_2$, Phys. Rev. B 88 (2013), 014423(11pp).